



A comparison of the parameters of the working elements of troweling discs with a diameter of 600 mm and four blades regarding the uniformity of troweling concrete surfaces

Jarosław Kalinowski¹

ABSTRACT:

The troweling process increases the functional properties of the treated concrete surface. The final troweling process is most often performed using disc trowels with four working elements in the form of blades similar in shape to a rectangle. In this work, a disc trowel with a diameter of 600 mm was selected as an example. Six commercially available blades with different geometries were compared in terms of machining uniformity. Through the simulation process, the values of geometric efficiency were determined for each type of blade and the optimal overlaps of the disc movement paths on the right and left sides were determined in order to obtain the best uniformity of machining determined by minimizing the standard deviation index ε of geometric efficiency S_g .

KEYWORDS:

troweling; concrete; geometric efficiency

1. Introduction

The final process of treating concrete surfaces is the troweling process. A properly and evenly performed troweling process results in a uniform increase in the strength and durability of concrete surfaces, reduces operating costs, and improves the aesthetic features of the surface. Troweling is usually performed with disc trowels. These types of trowels are characterized by a simple design, as well as a high reliability and efficiency [1-3]. This process involves smoothing the concrete surface using working elements made of steel sheet. This process is divided into a preliminary and finishing part. The initial part of troweling is performed using solid discs with a wheel geometry and a trowel radius R . Finishing troweling, often combined with rubbing in floor refining materials and is performed using working elements with rectangular or close to rectangular geometries. There are a large number of companies on the market offering trowels with various working diameters. For comparison, the article analyzes trowels with a diameter of 600 mm and working elements for surface finishing. These trowels are characterized by one of the smaller diameters, which is why they are often called edge trowels due to the easier possibility of working at the edges and corners of the floor limited by walls, where they minimize the size of the untroubled surface. Six working elements commercially available for this type of trowel were analyzed.

2. The principle of operating a disc trowel

A disc trowel consists of a drive system element used to rotate a disc with a troweling disc mounted on the rotating axis. The drive system loads the disc by transferring its weight through

¹ Czestochowa University of Technology, Faculty of Civil Engineering, ul. Akademicka 3, 42-218 Czestochowa, Poland, e-mail: jaroslaw.kalinowski@pcz.pl, orcid id: 0000-0001-8922-4788

the working elements to the processed surface. The heads of commercially available trowels consist of four brackets to which replaceable working elements are attached. Most trowels allow the brackets to be rotated by an angle of 0 to 15 degrees around the bracket axis. As the angle of inclination of the working elements increases, the pressure on the rear edge of the working element increases, which increases the processing efficiency in the case of a hardened concrete mixture. The full wheel-shaped working element is attached by inserting a trowel with four blades directly onto this element so that the blades rest on locks that prevent mutual rotation.

The impact of the trowel on the treated surface results from the simultaneous rotational movement of the disc and the translational movement of the entire trowel.

3. Types of commercially available work pieces

The analysis of working elements available on the market for trowels with a working diameter of 600 mm identified the six models presented in Figures 1 to 6. Figures 1 to 4 show rectangular blades with a mounting of half the width of the blade. Figures 1 and 2 show rectangular blades with different dimensions. The blades in Figures 3 and 4 have a geometry close to a rectangle, which can be obtained by cutting or bending the corners from a rectangular sheet. The working elements in Figures 5 and 6 have a mounting that is asymmetrical in relation to the blade width, closer to the leading edge, making their shape more complicated than the blades in Figures 1 to 4.

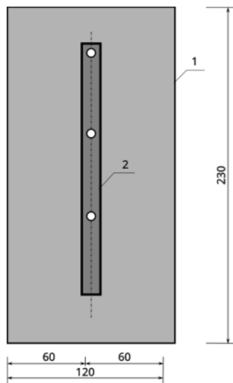


Fig. 1. Working element for 600 mm trowels from Pro-Masz, size 230x120 mm, 1 – surface of the working element, 2 – mounting

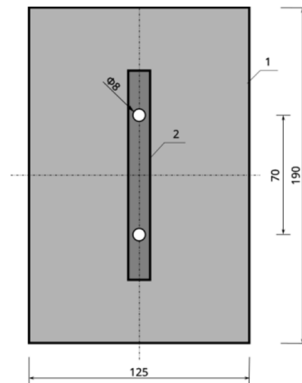


Fig. 2. Working element for M&M trowels, size 190x125 mm, 1 – surface of the working element, 2 – mounting

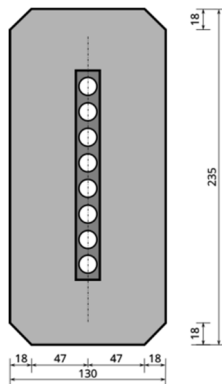


Fig. 3. Working element for Kreber K-600 E and B trowels, 1 - working element surface, 2 - mounting

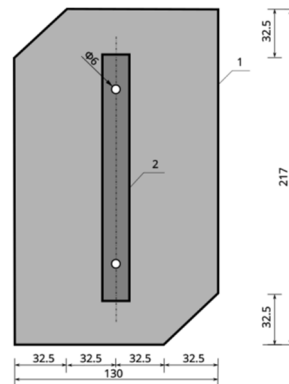


Fig. 4. Working element for Kreber K-600 E and B ver. 2 trowels, 1 – surface of the working element, 2 – mounting

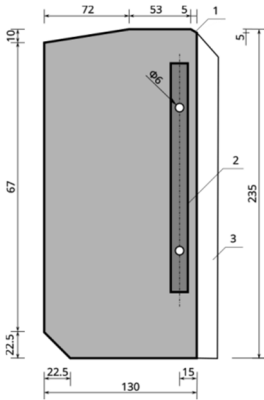


Fig. 5. Working element for Belle, Halcon, Enaro trowels, diameter 600 mm, size 235x130 mm, manufactured by Dysk Bud, 1 – surface of the working element, 2 – mounting, 3 – stiffening

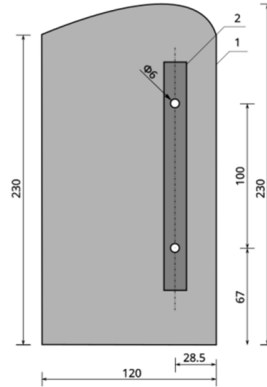


Fig. 6. Working element for Barikell trowels, model PALA 4-60, diameter 600 mm, 1 – surface of the working element, 2 – mounting

4. Determining the impact of the disc trowels on the treated surface

The trowel disc rotates around the axis and at the same time moves in a translational motion, sliding in the contact points which are the surfaces of the working elements on the treated surface. Each point of the machined surface draws a contact trajectory with the work elements on the work elements. The length of this trajectory is a quantitative measure of the processing intensity called the geometric efficiency S_g .

The geometric effectiveness of the working tool S_g at a given point on the machined surface is the length of the line of contact of the point with the surface of the working element after the working tool passes through this point. An example curve constituting the contact line of the machined point with the disc is shown in Figure 8.

4.1. Assessment of the uniformity of the shield's impact

A number of parameters depend on the value of the geometric effectiveness S_g , such as roughness and compressive strength of the near-surface concrete layer. The uniformity of S_g is correlated with the uniformity of the distribution of other physical parameters. Ensuring uniform processing by ensuring uniform physical parameters of the concrete surface increases the quality of processing while reducing the amount of energy needed for processing.

For n values evenly distributed over the measurement section, the uniformity of the S_g impact distribution is determined by the standard deviation index ε , calculated by the formula:

$$\varepsilon = \frac{\sigma_{S_g}}{\bar{S}_g} = \sqrt{\frac{\frac{1}{2}(S_{g1} - \bar{S}_g)^2 + \sum_{i=2}^{n-1}(S_{gi} - \bar{S}_g)^2 + \frac{1}{2}(S_{gn} - \bar{S}_g)^2}{\bar{S}_g^2(n-1)}} \quad (1)$$

5. Methodology for simulating the impact of a disc trowel on the treated surface

The simulation of the impact of the disc on the processed surface was performed based on the following objects: Disc, Track, Sensors, Simulation.

The disc object contains objects that define the surfaces of work items in the form of polygons. The basic methods of this object allow you to move and rotate the disc and check whether the coordinates of a given point coincide with the surface of the working element.

The track object contains the parameters of the disc movement, i.e. the initial and final parameters of the movement by coordinates, as well as the translational and rotational velocities. Using interpolation, the method determines the position of the disc center, the translational velocity vector and the rotational speed for time t .

The sensors object is a base of point coordinates in which we calculate the geometric effectiveness of S_g . The basic methods of this object allow you to save and read the values of point coordinates and S_g values, and perform statistical operations such as the standard deviation indicator.

The simulation object for each time t in fixed time intervals dt sets the disc and for each sensor checks whether its position coincides with the working element. It calculates the vector sum of the translational speed and the speed resulting from the rotational movement of the disc according to formula (2). The product of the calculated speed and the time step dt is the value of the geometric efficiency in the time step by which the sensor value is modified. After traversing the entire route defined by the track object, the sensors object contains S_g values for the tested points.

The resultant speed V_w resulting from the translational speed V_p and rotational speed ω of the disc for point $P(x, y)$ in the local coordinate system of the disc as in Figure 7 is given by the formula:

$$V_w(x, y) = \sqrt{V_p^2 + 2V_p x \omega + y^2 \omega^2 + x^2 \omega^2} \tag{2}$$

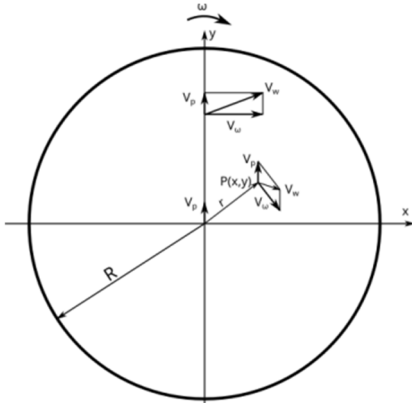


Fig. 7. Determining the resultant speed for the disc at point $P(x, y)$, which is the sum of the translational speed V_p and the linear speed V_ω resulting from the rotational speed ω [4]

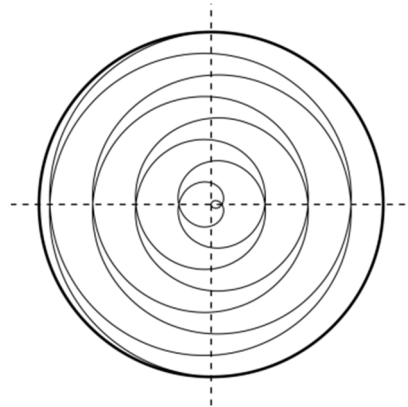


Fig. 8. An example curve drawn by the point of the machined surface at the center of the machining on a moving disc with an angular velocity of $\omega = 4.189$ rad/s and a translational velocity of $V_p = 0.1$ m/s

$$dS_g = V_w(t) \cdot dt$$

$$y(t) = R - V_p \cdot t$$

$$V_w(t) = \sqrt{V_p^2 + 2V_p x \omega + (R - V_p \cdot t)^2 \omega^2 + x^2 \omega^2}$$

$$V_w(t) = \sqrt{V_p^2 + 2V_p x \omega + R^2 \omega^2 - 2R \cdot V_p \cdot t \omega^2 - V_p^2 t^2 \omega^2 + x^2 \omega^2} \tag{3}$$

For a solid shield, when $x^2 + y(t)^2 > R^2$ the sensor is outside the shield's impact range, the geometric effectiveness value $dS_g = 0$ [5, 6].

6. Construction of trowel disc models according to the geometry of the working elements

Modeling the disc for numerical calculations involves locating the geometry of the working elements relative to the center of the disc. Work elements are modeled using polygons by specifying the coordinates of their vertices in the local coordinate system whose origin is the axis of rotation of the disc. Specifying the coordinates of one work item allows you to determine the position of the other work items by performing a rotation or symmetric reflection operation.

The working elements are located in the disk in such a way that the outermost vertices are at a distance R from the center of the disc. The R value defines the radius of the disc.

6.1. Rectangular working elements with symmetrical mounting

The geometry diagram of the disc with four working elements in the form of rectangles is shown in Figure 9. The symmetrical mounting of the blades makes the entire system symmetrical along the coordinate axes.

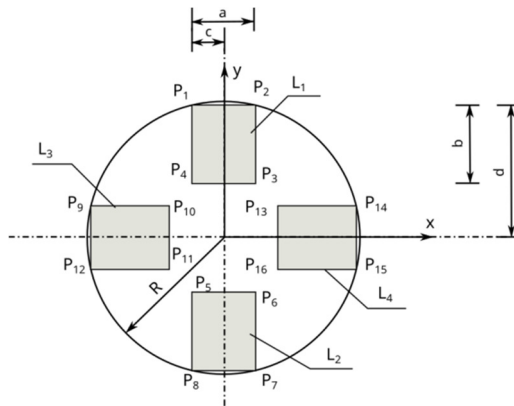


Fig. 9. Diagram of a troweling disc consisting of four rectangular working elements (L_1, L_2, L_3, L_4) with the tops of the working elements marked ($P_1 \dots P_{16}$)

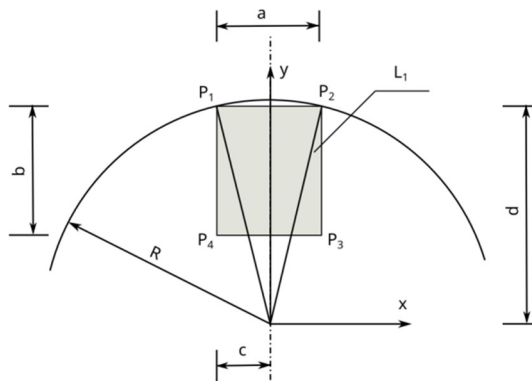


Fig. 10. Scheme for determining the location of the coordinates of the vertices of the rectangular upper blade (L_1)

The coordinates of the rectangular blade L_1 with blade width a and height b inscribed in a circle with disk radius R can be determined based on Figure 10.

The coordinates of the points $P_1, (-c; d), P_2(c; d)$ of the external corners of the blade with width a can be calculated using the following formulas:

$$c = \frac{a}{2}d = \sqrt{R^2 - \frac{a^2}{4}} \quad (4)$$

The remaining points have the following coordinates $P_3(c; d-b)$, $P_4(-c; d-b)$. The coordinates of the remaining blades L_2, L_3, L_4 can be determined using the symmetry with respect to the L_1 blade. The coordinates of the tips of all blades are included in Table 1.

Table 1
Coordinates of the blade tips according to Figures 1-3

Position of the working element	Designation of the working element	Coordinates of the blade corners			
top	L_1	$P_1(-c; d)$	$P_2(c; d)$	$P_3(c; d-b)$	$P_4(-c; d-b)$
bottom	L_2	$P_5(-c; b-d)$	$P_6(c; b-d)$	$P_7(c; -d)$	$P_8(-c; -d)$
left	L_3	$P_9(-d; c)$	$P_{10}(b-d; c)$	$P_{11}(b-d; -c)$	$P_{12}(-d; -c)$
right	L_4	$P_{13}(d-b; c)$	$P_{14}(d; c)$	$P_{15}(d; -c)$	$P_{16}(d-b; -c)$

6.2. Rectangular working elements with cut-out corners and symmetrical mounting

In the case of selected exemplary working elements, the blades in Figures 3 and 4 were considered. In the case of the blade from Figure 3, the coordinates of the blade vertices L_1 located on the disc circumference can be calculated as in point 6.1, substituting the distance between these points into the formula for a . In the case of the blade in Figure 4, the coordinate of the upper right tip of the blade L_1 located on the circumference of the disc can be calculated as in point 6.1, substituting the width of the blade into the formula for a . We calculate the remaining coordinates of the vertices using the distances between the vertices dimensioned in the drawings or the symmetry of the blade position relative to the axis of the coordinate system.

6.3. Working elements with complex geometry

The location of the working elements in Figures 5 and 6 with more complex geometries was determined numerically. This method was particularly applicable to the blade geometry in Figure 6, where the arc geometries were approximated using short sections.

The algorithm consisted in positioning the L_1 element in the disc so that the blade assembly axis coincided with the vertical axis of the disc, and the lower edge coincided with the X axis. By moving the blade figure vertically and calculating the maximum distance of any vertex of the figure from the center of the disc using the half-interval method, the vertical shift of the blade relative to the initial position was determined with numerical accuracy. The position of the remaining blades was determined by rotating the L_1 blade by 90, 180 and 270 degrees.

7. Simulation results of the impact of a disc trowel on the treated surface

The simulation assumed discs with a radius of $R = 300$ mm with working elements according to six patterns from Figures 1 to 6, moving with a disc rotational speed of $\omega = 4.189$ rad/s (80 revolutions per minute) and a translational speed of $V_p = 0.1$ m/s.

The assumed length of the sensor line was the size of the disc diameter $l = 600$ mm with a constant spacing of 1 mm and the time step size $dt = 0.0001$ s. The value of geometric efficiency S_g was determined for a single pass of the disc and with optimal overlaps on the right and left sides so as to obtain the highest uniformity of machining, expressed by the standard deviation index ε . The charts for individual discs with built-in working elements from Figures 1 to 6 are shown in Figures 11 to 16, respectively. Detailed values of the geometric efficiency S_g ,

the standard deviation index ε and the size of the overlaps on the left and right sides are presented in Table 2.

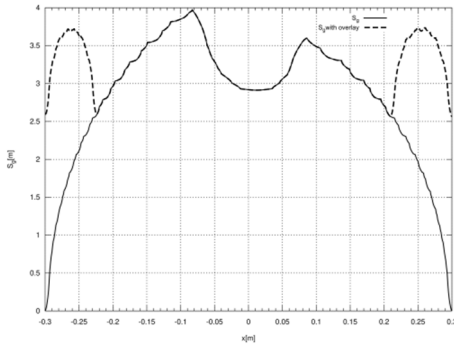


Fig. 11. Diagram of geometric efficiency for a single pass of the disc and with overlays for a disc with four blades with geometry as shown in Figure 1 (disc 1)

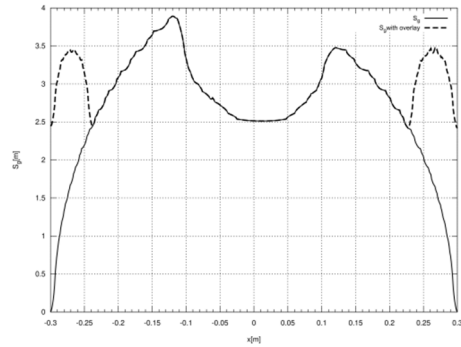


Fig. 12. Diagram of geometric efficiency for a single pass of the disc and with overlays for a disc with four blades with geometry as shown in Figure 2 (disc 2)

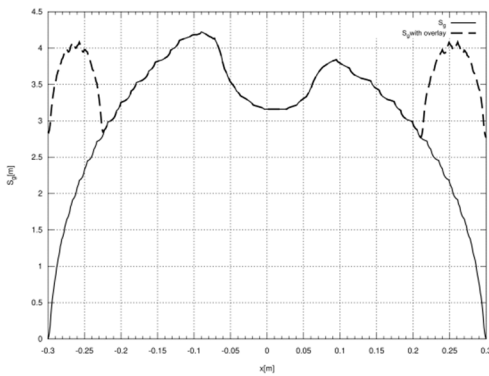


Fig. 13. Diagram of geometric efficiency for a single pass of the disc and with overlays for a disc with four blades with geometry as shown in Figure 3 (disc 3)

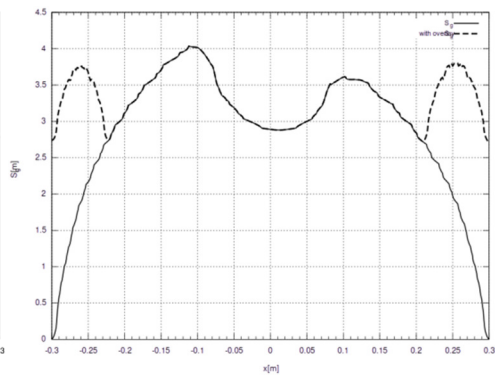


Fig. 14. Diagram of geometric efficiency for a single pass of the disc and with overlays for a disc with four blades with geometry as shown in Figure 4 (disc 4)

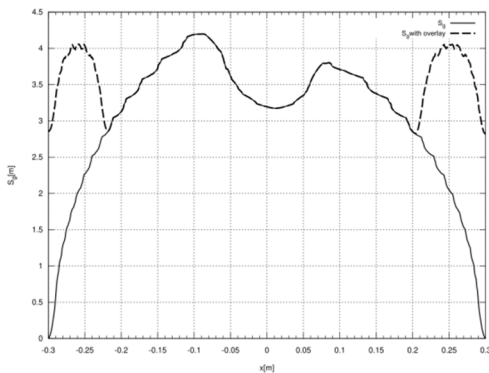


Fig. 15. Diagram of geometric efficiency for a single pass of the disc and with overlays for a disc with four blades with geometry as shown in Figure 5 (disc 5)

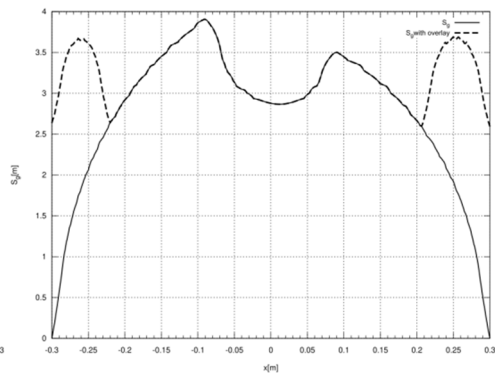


Fig. 16. Diagram of geometric efficiency for a single pass of the disc and with overlays for a disc with four blades with geometry as shown in Figure 6 (disc 6)

Table 2

Grinding parameters for a single disc pass and with optimal overlaps

Type of disc	Single disc pass		Disc transition with overlays			
	S_g [m]	ε	S_g [m]	ε	a [m]	b [m]
Disc 1	2.81246	0.300688	3.28788	0.107192	0.0764051	0.0903413
Disc 2	2.67331	0.291217	3.02777	0.131241	0.0622719	0.0724709
Disc 3	3.05172	0.297711	3.56667	0.104964	0.0765038	0.089534
Disc 4	2.85512	0.316886	3.33959	0.107325	0.0784797	0.0913921
Disc 5	3.01565	0.315095	3.56279	0.103985	0.0823018	0.0964632
Disc 6	2.75088	0.309476	3.23355	0.104453	0.0795656	0.0934773

a – size of the overlay on the left side, b – size of the overlay on the right side

8. Conclusions

The paper presents an analysis of the troweling effectiveness of working elements for four-blade disc trowels with a diameter of 600 mm. Six commercially available working elements with a nearly rectangular geometry were selected and used for final troweling. These were working elements made by trowel manufacturers as well as substitutes made as universal blades by independent producers. All geometries were rectangular or close to rectangular. The modifications consisted of rounding or removing corners. In the case of a single pass of the target, the obtained geometric efficiencies S_g ranged from 2.67331 m for disc 2 to 3.05172 m for disc 3. The value of the standard deviation index for these discs was the smallest and amounted to 0.291217 and 0.297711, respectively. The highest value of the indicator was 0.316886 for disc 4. The results indicate disc 3 as the most suitable for edge grinding due to the highest efficiency and a small standard deviation index compared to other discs, which indicates a high rate of increase of the S_g value at the machining edge. This is due to the symmetrical cutting of the corners of the blade rectangle in Figure 3, which allows a larger surface of the working element to work closer to the circumference of the disc.

In the case of analyzing the operation of the disc with overlapping, S_g values were achieved from 3.02777 m for disc 2 to 3.56667 m for disc 3. The standard deviation values ranged from 0.103985 for disc 5 to 0.131241 for disc 2. The standard deviation index for disc 3 is 0.104964, it is the third in order and is not much different from the minimum value.

The simulations performed indicate disc 3 with working elements from Figure 3 as the most universal, which gives favorable results both with single edge grinding and with overlays.

References

- [1] Chrzyszczewski W., Obróbka mechaniczna i obrabiarki do kamienia, h.g.BRAUNE, Jawor 2004.
- [2] Tyrowicz T., Kamieniarstwo, Obróbka maszynowa, Arkady, Warszawa 1958
- [3] Rajczyk J., Podstawy naukowe doboru struktury i kinematyki tarczowych narzędzi roboczych maszyn do obróbki powierzchni betonu, Wydawnictwo Politechniki Częstochowskiej, Częstochowa 2007.
- [4] Respondek Z, Rajczyk Z, Kosiń M., Jończyk D., Kalinowski J., A new method of constructing a disc for concrete surface floating, Advanced Materials Research, Xiamen 2013, 97-104.
- [5] Kalinowski J., The optimization of kinematic and geometric parameters in two-element grinding discs with a central rotational axis for the uniformity of concrete surface treatment, Zeszyty Naukowe Politechniki Częstochowskiej 2019, 175, Budownictwo 25, 78-85.
- [6] Kalinowski J., Optimization of kinematic and geometric parameters in three-element grinding discs with a central rotational axis for the uniformity of concrete surface treatment, Zeszyty Naukowe Politechniki Częstochowskiej 2020, 176, Budownictwo 26, 66-75.

Porównanie parametrów elementów roboczych tarcz zacierających o średnicy 600 mm z czterema łopatkami ze względu na równomierność zacierania powierzchni betonowych

STRESZCZENIE:

Proces zacierania powoduje zwiększenie właściwości użytkowych obrabianej powierzchni betonowej. Końcowy proces zacierania wykonuje się najczęściej za pomocą zacieraczek tarczowych z czteroelementowymi elementami roboczymi w postaci łopatek zbliżonych w kształcie do prostokąta. W pracy jako przykład wybrano zacieraczkę tarczową o średnicy 600 mm. Porównaniu poddano sześć łopatek o różnych geometriach dostępnych w handlu pod względem równomierności obróbki. Poprzez proces symulacji wyznaczono wartości skuteczności geometrycznej dla każdego rodzaju łopatek oraz wyznaczono optymalne nakładki torów ruchu tarczy z prawej i lewej strony tak, aby uzyskać najlepszą równomierność obróbki określoną przez minimalizację wskaźnika odchylenia standardowego ε skuteczności geometrycznej S_g .

SŁOWA KLUCZOWE:

zacieranie; beton; skuteczność geometryczna